

## PHOTO-PHYSICAL AND MORPHOLOGICAL STUDIES OF ORGANICALLY PASSIVATED CORE-SHELL ZnS NANOPARTICLES

Manoj Sharma<sup>\*</sup>, Sunil Kumar<sup>a</sup>, O.P.Pandey  
*School of Physics and Materials Science, Thapar University, Patiala, India*  
*<sup>a</sup>Department of Physics, Maharishi Markandeshwar University, Mullana, India*

In this paper we have reported the synthesis of luminescent nanoparticles of Zinc Sulfide (ZnS) with and without capping agent. Nanoparticles of ZnS are prepared by a coprecipitation reaction. Based on Ostwald ripening and surface passivation, we discuss a mechanism for the formation of ZnS nanoparticles. The reaction proceeds with the nucleation of ZnS crystals, which are immediately passivated by the anions in the solution. This in turn attracts cations including Zinc and which contribute to the growth of the crystal. These nanoparticles are sterically stabilized using organic polymer Poly Vinyl Pyrrolidone (PVP). The change in optical and morphological properties of ZnS nanoparticles is observed by using organic capping agent. The nanoparticles are of 6–8 nm in diameter as from TEM, each containing primary crystallites of size 2.2nm that were estimated from the X-ray diffraction patterns. Band gap measurements done by UV-visible spectrophotometer and excitation spectra shows that band gap increases by introducing capping material. Photoluminescence studies shows that emission intensity increases for capped sample. The nano core-shell ZnS will be a very suitable material for any type of optoelectronic application as we can control various parameters in this case in comparison to the uncapped nanostructures. .

(Received August 19, 2008; accepted August 22, 2008)

*Keywords:* Capping, uncapped, Bandgap, Excitation, Emission, PVP

### 1. Introduction

Semiconductor nanoclusters or quantum dots (QDs) exhibit size dependent properties [1-8]. Since these nano quantum dots have very high surface to volume ratio so surface defects play an important role in their study. The conventional approach for synthesis of nanoparticles involves chemical or physical attrition from bulk into objects of desired sizes and shapes (e.g. mechanical milling, ion implantation, etc.), and is referred as the 'top-down' approach. Inverse to the 'top-down' approach is a process universal in nature, involving the assembly of materials from molecular levels to form micro or macro-sized shapes and structures, often referred as 'bottom-up' approach or 'self-assembly' [8]. Wet chemical synthesis involving colloids is the most energy efficient 'bottom up' technique for the synthesis of nanoparticles. The chemical synthesis has the advantages of producing size-controlled, un-agglomerated nanoparticles. The tunability of the properties of nanoparticles by controlling their size may provide an advantage in formulating new composite materials with optimized properties for various applications. But applications of these materials are restricted due to different non-radiative relaxations pathways [6-8]. One important non-radiative relaxation is surface related defects. Most of the physical or chemical properties exhibited by these nanoparticles are due to their crystallites. Further growth in their size is due to agglomeration of these crystallites to form primary particles. If this growth of particles is not controlled, then due to Ostwald ripening and Vander-Waals interactions between particles, they agglomerate and settle down [6-8]. This agglomeration can be arrested by either stabilizing them

---

\* Corresponding author : manojnarad@gmail.com

electrostatically or by inducing steric hindrance at appropriate stages to achieve size selective synthesis during precipitation reaction.

Electrostatic stabilization involves the creation of an electrical double layer arising from ions adsorbed on the surface and associated counter ions that surround the particle in the dispersing media. Thus, if the electric potential associated with the double layer is sufficiently high, coulombic repulsion between the particles will prevent their agglomeration. Steric hindrance can be achieved by the adsorption of large molecules such as polymers on the surface of the particles. In order to control the growth one can use different organic and inorganic capping agents to passivate the free QD's. To control the growth of nanoparticles organic stabilizers (polymers) e.g. polyethylene oxide (PEO), poly(N-vinyl-2pyrrolidone)(PVP), Polyvinyl carbazole(PVK), mercaptoethanol, thiophenol, thiourea, SHMP, sodium polyphosphate, chitosan etc. can be added during the wet chemical synthesis for capping [12-19, 28]. Such materials have applications in luminescent devices, light emitters, phosphors optical sensors etc. [9-11]. Recently due to advancement in luminescent nanocrystals by successful capping which results in fluorescent labeling by semiconductor QD's for biological detection and tagging has demonstrated its application in many fields[20-25]. Capping causes noticeable change of properties of nanoparticles[26,27]. Here in this paper, Core-Shell ZnS nanoparticles have been synthesized, using chemical precipitation methods. Optical and morphological measurements on ZnS nanoclusters have been carried out to investigate surface effects along with quantum size effects.

## **2. Experimental**

Zinc sulphide (ZnS) nanoparticles were synthesized by chemical precipitation method. Homogeneous solutions of zinc acetate and sodium sulphide were prepared in an aqueous media. 0.5 M zinc acetate ( $\text{Zn}(\text{CH}_3\text{COO})_2 \cdot \text{H}_2\text{O}$ ) solutions and 0.5 M sodium sulfide solution were used for synthesis of ZnS nanoparticles. As a capping agent poly (N-vinyl-2pyrrolidone) (PVP) was also added to the reaction medium i.e. for controlling the particle size. First, no surface-capping agent has been used for the stabilization of the nucleated particles; instead, the nanoparticles are allowed to interact freely in the aqueous medium. In the second attempt PVP (2 % at. wt) was added in 0.5 molar zinc acetate and then 0.5 M sodium sulphide was added drop wise. The precipitate appears soon after the addition of sodium sulphide ( $\text{Na}_2\text{S}$ ). The stirring was further allowed for 15 minutes at room temperature using a magnetic stirrer. The precipitated particles were filtered using whatman 40 filter paper. To remove the last traces of adhered impurities, the particles were washed several times using double distilled water. The washed particles were dried at 60°C in air.

### **2.1 Morphological and Optical Characterization**

The ZnS nanoparticles were characterized by X-ray diffraction (XRD) using Rigaku, model D-maxIIIIC diffractometer with  $\text{Cu K}\alpha$  radiation. TEM studies were conducted using a Transmission Electron Microscope, Hitachi (H-7500) 120 kV equipped with CCD Camera. This instrument has the resolution of 0.36 nm (point to point) with 40-120 kV operating voltage and can magnify object up to 6 lakh times in high resolution mode. Optical reflectance of the ZnS particles were recorded with an double beam UV-Visible spectrophotometer (Model: Hitachi - 330) in the range 220–800 nm. The instrument has also integrating sphere to analyze the powder samples in the 200 nm to 800 nm range and a specular reflectance accessory to study reflective surfaces. PL studies were done by Fluoramax-3 spectrofluorometer.

### 3. Results and Discussions

#### XRD Results

The XRD pattern of synthesized capped and uncapped powder is shown in fig-1. Both shows three broad peaks corresponding to the (111), (220) and (311) planes.

Crystallite size of ZnS nanoparticles was calculated by following Scherrer's equation,

$$D = k\lambda / \beta\cos\theta \quad (1)$$

where  $k=0.9$ ,  $D$ - crystallite size ( $\text{\AA}$ ),  $\lambda(\text{\AA})=1.54$  be the wavelength of Cu  $K\alpha$  radiation and  $\beta$ -corrected half width of the diffraction peak. The average crystallite size calculated from these peaks using Scherer's formula is 2 nm. Three peaks have been observed in the span ranging from  $5^\circ$  to  $100^\circ$ . Lattice planes corresponding to above mentioned peaks have been identified by applying extinction rules. The ratios corresponds to FCC structure. It is to be noted that, the peaks observed in the XRD patterns match well with those of the  $\beta$ -ZnS (cubic) reported in the JCPDS Powder Diffraction. Intensities of the three most important peaks of ZnS, namely  $\langle 111 \rangle$ ,  $\langle 220 \rangle$  and  $\langle 311 \rangle$  reflections corresponding to  $28.5^\circ$ ,  $47.6^\circ$  and  $56.4^\circ$  respectively do not deviate from the Powder Diffraction File intensities. Broadening of the XRD peaks both in capped and uncapped samples indicates the formation of ZnS nanocrystals. Elongation of the XRD pattern in case of capped nanoparticles also shows the surface passivation.

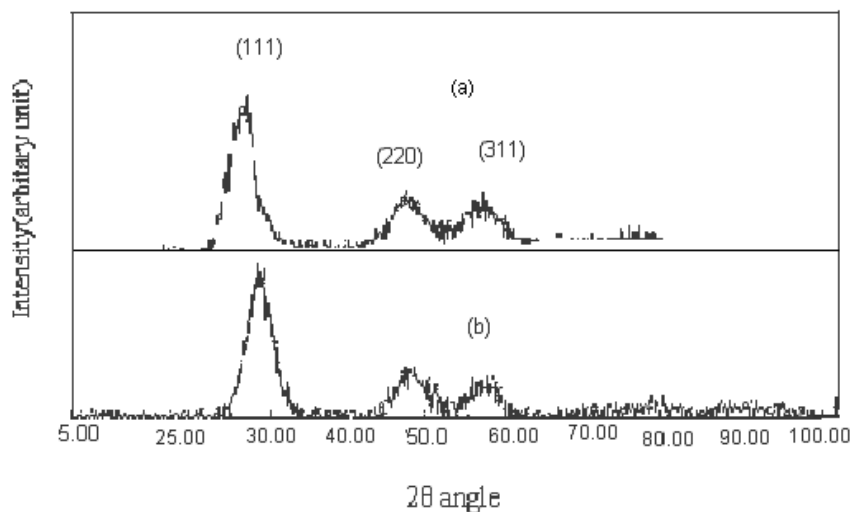


Fig-1- XRD pattern of and uncapped (a) and (b) PVP capped ZnS nanoparticles.

#### TEM results

The TEM results of the synthesized powders are shown in fig. 2. It is clear that PVP capped nanoparticles are unagglomerated (fig.2a) and uncapped are agglomerated (fig.2b). ZnS core shell nanoparticles are capped with organic PVP layer that hinders agglomeration both sterically and electrostatically. Inorganic core and organic shell ZnS nanoparticles are better passivated with shell layer that seize nucleation at very early stage and can passivate surface defects or dangling bonds.

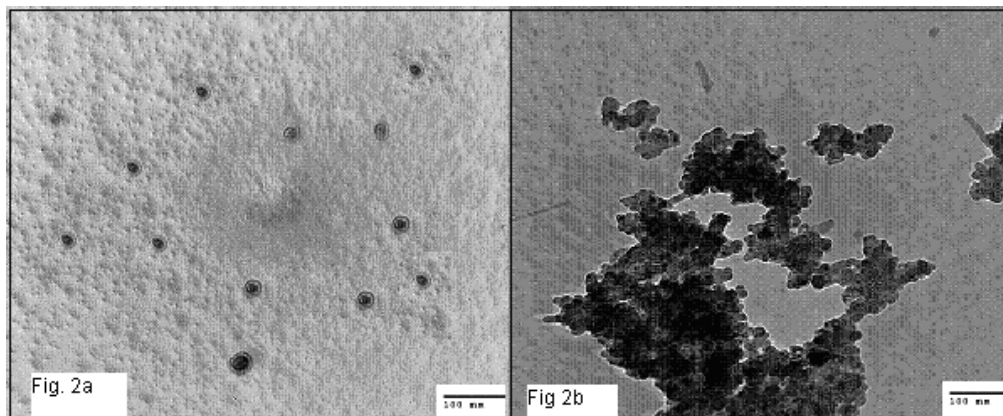
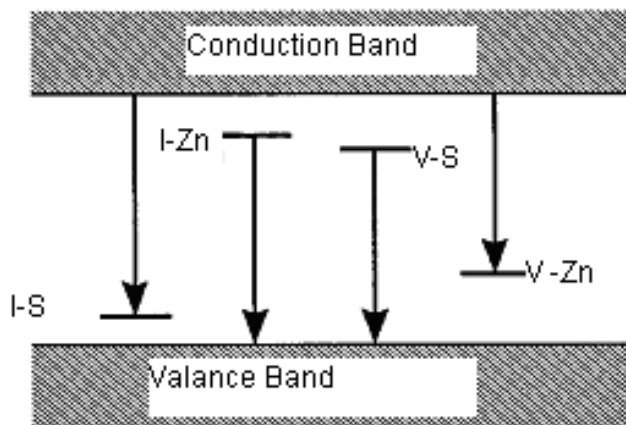


Fig-2. TEM of PVP capped ZnS nanoparticles (Fig-2a) and uncapped ZnS nanoparticles (Fig-2b).

### PL Studies

Excitation peak (Fig-4) of ZnS capped with PVP 2% at wt. have absorption edge is at 280nm. Bandgap of the nanoparticles ( $E=hc/\lambda$ ) is found to be 4.42 eV where as for uncapped samples excitation peak is at 305nm showing band gap to be 4.06eV which clearly shows quantum size effects (where  $E$  is Band gap energy,  $h$  is planck's constant,  $c$  is velocity of light,  $\lambda$  is wavelength). It has been reported in previous work on colloidal ZnS that vacancy states lie deeper in the gap than states arising from interstitial atoms [15]. Therefore we conclude that the two long 440 and 453 nm and the two short 412 and 423 nm wavelength peaks are due to transitions involving vacancy states and interstitial states, respectively shown in Fig-3. The other peaks 468nm, 483nm and 561nm are reported here first time. The emission spectra shows that the emission intensity of capped ZnS nanoparticles is comparatively high in comparison to uncapped ZnS nanoparticles which shows dangling bonds are better passivated in PVP capped nanoparticles in comparison to uncapped ZnS nanoparticles. This is expected because in the absence of capping agent uncontrolled nucleation and growth of the particles occurred, resulting in the formation of defect states. From Fig-5 it is clearly shown that there is considerable increase in intensity of emission peaks of PVP capped ZnS nanoparticles (412nm, 440nm, 468nm, 483nm, 561nm) as compared to uncapped ZnS nanoparticles. This is attributed due to transfer of energy from chemisorbed PVP molecules to interstitial sites and vacancy centers. So enhanced photoluminescence has been observed from the ZnS nanocrystals due to efficient energy transfer from the surface adsorbed PVP molecules to interstitial and vacancy centers in nanocrystals. This study brings out a sensitizer (energy donor)—activator (energy acceptor) type relation between the polymeric capping agent and luminescent semiconducting nanoparticles. Manzoor et al. [27] have shown energy transfer from polymer layer to dopant centers. But as undoped ZnS nanoparticles also shows PL. It is found that transfer of energy takes place from PVP energy levels to zinc and sulfur states (native or defect related). G Ghosh et al. [28] also have shown increase in PL intensity of capped ZnS nanoparticles in comparison to uncapped ZnS nanoparticles. But to the best of our knowledge no one have reported increase in PL intensity of uncapped ZnS as well as transfer of energy from chemisorbed polymers to interstitial sites or vacancies. Also if we add dopants to our PVP capped ZnS samples they can take place of sulphur vacancies and  $Zn^{2+}$  surface states and can get desired colors with high intensity as compared to uncapped ZnS which clearly shows need of capping agents.



*Fig-3 Transitions in ZnS*

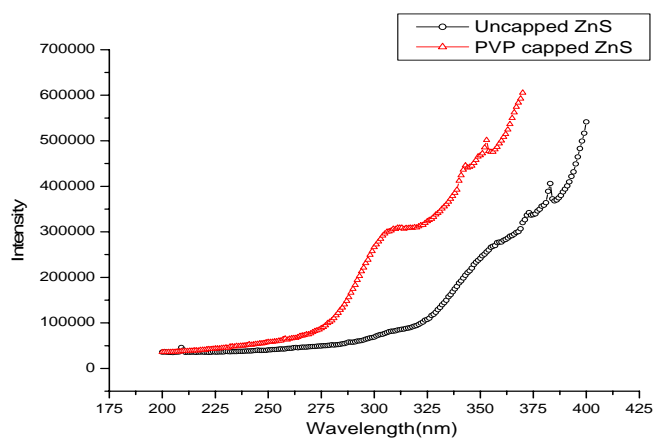


*Fig-4 Excitation spectra of ZnS capped with PVP 2% at wt*

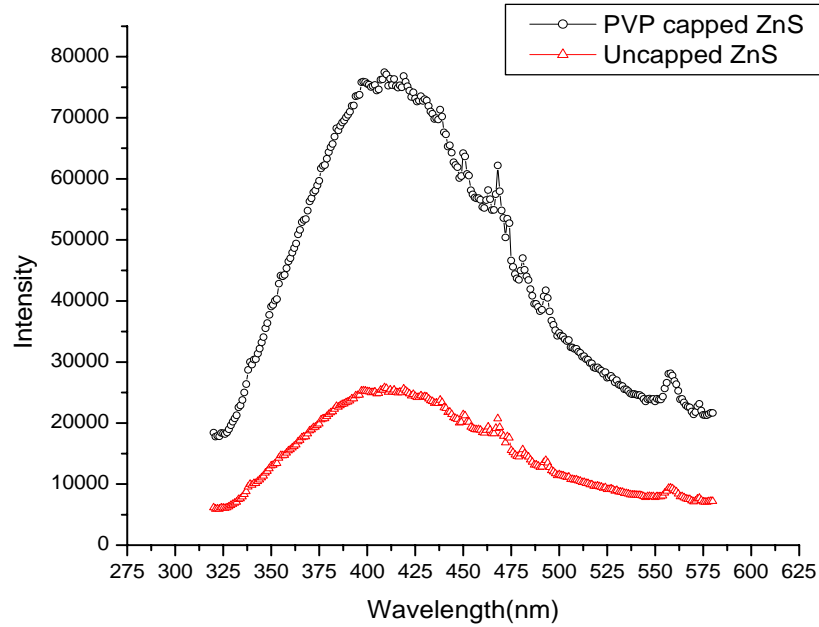


Fig-5 Emission spectra of PVP capped and uncapped ZnS nanoparticles

### UV visible Reflectance spectra

Uncapped ZnS nanoparticles have absorption edge (Fig-6) at 297nm and PVP capped ZnS nanoparticles have absorption edge at 280 nm. So band gap of PVP capped ZnS nanoparticles comes out to be 4.42 eV and for uncapped ZnS nanoparticles it is 4.17eV. Bandgap of the nanoparticles is calculated from

$$E = hc/\lambda \quad (2)$$

where E is Band gap energy, h is planck's constant, c is velocity of light,  $\lambda$  is wavelength of absorption edge in reflectance spectra.

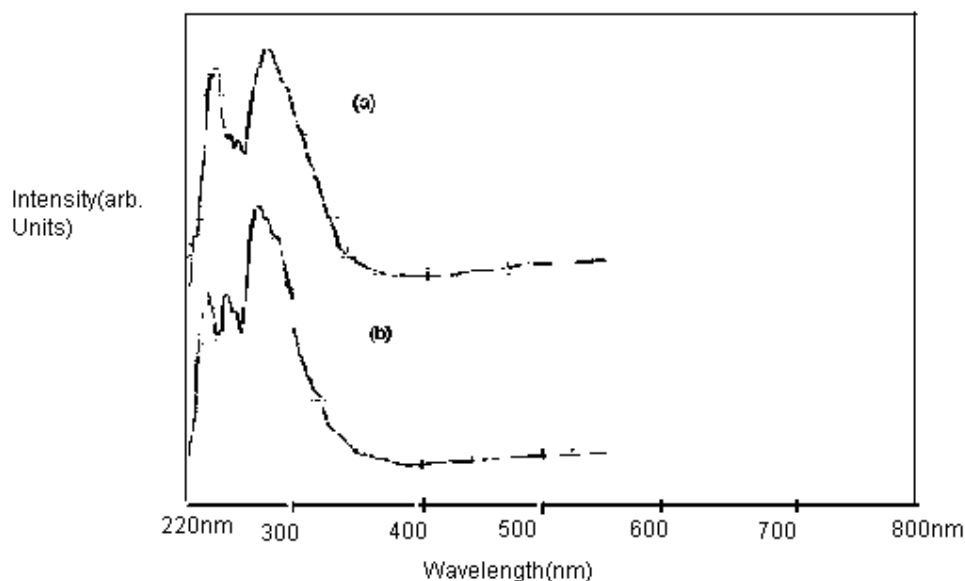


Fig-6 Reflectance spectra of ZnS nanoparticles (a) uncapped (b) PVP capped.

Zinc acetate dissociates into zinc ions ( $Zn^{2+}$ ) and acetate ( $Ac^-$ ) ions in aqueous solution. Similarly sodium sulfide dissociate into its respective cations and anions [27,29]. Sodium being more reactive than zinc readily forms sodium acetate. Particles of ZnS nucleate due to the reaction between  $Zn^{2+}$  and  $S^{2-}$ , which subsequently grow by consuming more ions from the solution. The growth mechanism can be explained on the basis of Ostwald ripening [10]. Upon nucleation, the surface energy of the particles is very high and consequently the surface is passivated by adsorption of anions in the solution ( $Ac^-$  and  $S^{2-}$ ). The accumulation of anions in turn attracts cations ( $Zn^{2+}$  and  $Na^+$ ) towards the surface of the particle.  $Zn^{2+}$  reacts with  $S^{2-}$  and gets incorporated into the crystal lattice of the nucleus. Eventually enough  $Na^+$  accumulates (sodium is not known to form alloys with zinc) to repulse  $Zn^{2+}$  ions from approaching the particle surface and the particle growth stops [29]. These accumulated  $Na^+$  ions form the stern layer over ZnS nanoparticles, attracting  $Ac^-$  ions to form a diffuse layer over it. In this way, the particle growth is completely stopped. To avoid further agglomeration, a repulsive force must be added between the particles to balance the attractive forces. This is achieved by adsorbing a layer of polymer over nanoparticles inducing steric hindrance by employing PVP as the stabilizing agent. So in our uncapped ZnS sample only electrostatic stabilization is responsible for controlling agglomeration but in PVP capped samples besides electrostatic stabilization steric hindrance of polymer layer of adsorbed PVP also hinders nucleation which is well explained with high emission intensity of PVP capped ZnS in comparison to uncapped ZnS. So increased zeta potential due to electric double layer and adsorbed polymer gives unagglomerated nanoparticles. So we report better passivation of defects and dangling bonds in PVP capped ZnS nanoparticles in comparison to uncapped ZnS. Because of the easy dispersion of the PVP-ZnS composites, highly photo-luminescent polymer nanocomposites can be prepared by embedding these particles in transparent plastic media. Further, compositing with semiconducting polymers, organic-quantum dot hybrid electroluminescent displays can also be realized from these nanoparticles [27].

## Conclusions

Core-Shell ZnS nanocrystals have been synthesized using chemical precipitation method. Optical and morphological measurements on ZnS nanoclusters have been carried out to investigate the effect of capping on ZnS nanoparticles. XRD results show the crystallite size to be from 1.5-2.5 nm depending upon the peaks. TEM results shows uncapped agglomerated nanoparticles as

well as PVP capped ZnS particles. It is clear from the TEM that PVP capping forms core-shell nanostructures and they also avoid agglomeration of the particles. Band gap of PVP capped ZnS nanoparticles is found to increase in comparison with uncapped ZnS nanoparticles indicating quantum size effects. The bandgap data from UV-visible reflectance and excitation are in correlation with each other. Increase of intensity in case of capped ZnS compared to uncapped ZnS shows better surface passivation. In conclusion PVP layer leads to the transfer of energy to the possible transition levels in ZnS. It means we can synthesize highly efficient doped ZnS using this transfer mechanism.

### Acknowledgements

The authors thank to SAIF Panjab University Chandigarh for helping in recording TEM images of the samples and UV- visible spectra. The authors also thank Prof. Aggarwal of Dept. of Physics, Kurukshetra University, for their help in recording the Photoluminescence spectra.

### References

- [1] Al. L. Efros, A. L. Efros, *Sov. Phys. Semicond.*, **16**, (1982) 772.
- [2] L. E. Brus, *J. Chem.Phys.*, **80**, (1984) 4403.
- [3] Alivisatos AP, Harris TD, Carroll PJ, Stiegerwald ML, Brus LE, *J Chem. Phys.*, **90**, (1989) 3463.
- [4] Suchita Kalele, S. W. Gosavi, J. Urban and S. K. Kulkarni, *Current Science*, **91**, (2006) 8.
- [5] Matijevic. E, *Monodispersed colloids: Art and Science. Langmuir*, **2**, (1986)12–20.
- [6] Everett, D. H, *Basic principles of Colloid Science*, Royal Society of Chemistry, (1988).
- [7] Chung Jaehun, LEE Sunbae, Jang Du-Jeon, *Korea- Japan Forum, Seoul, Coree, Republicuede*, **377**, (2002) 85-88.
- [8] T. Kubo, T. Isobe, M. Senna, *Journal of Luminescence* **99**, (2002) 39–45.
- [9] H.C. Warad, S.C. Ghosh, A Sugunan, C. Thanachayanont, J. Dutta., *Advances in Technology of Materials and materials processing Journal (ISSN 1440-0731)*.
- [10] Benjamin Gilbert, Feng Huang, Zhang Lin, Carmen Goodell, Hengzhong Zhang, Jillian F. Banfield, *Nano Lett.*, **6**(4), (2006) 605-610.
- [11] H.C. Warad, S.C. Ghosh, B. Hemtanon, C. Thanachayanont, J. Dutta, *Science and Technology of Advanced Materials*, **6**, (2005) 296–301.
- [12] Dongjin Kim, Ki-Deuk Min, Jongwon Lee, Jeong Ho Park and Jong Han Chun, *Materials Science and Engineering: B*, **131**, (2006) 13-17.
- [13] Murray, C. R. Kagan, *Annu. Rev. Mater. Sci.* **30**, (2000) 545.
- [14] Qu, L., Z. A. Peng, *Nano Lett.* **1**, (2001) 333-337.
- [15] Bruchez, M. P., M. Moronne, *Science* **281**, (1998) 2013.
- [16] Chan W. C. W, S. Nie, *Science* **281**, (1998)2016.
- [17] Michalet, X, F. F. Pinaud, *Science* **307**, (2005) 583-544.
- [18] Y. Cao and U. Banin, *J. Am. Chem. Soc.* **122**, (2000)9693.
- [19] Dabbousi, B. O., J. Rodriguez-Viejo, *J Phys. Chem. B*, **101**, (1997) 9463.
- [20] Peng, X., M. C. Schlamp, **11**, (1997) 7019.
- [21] Reiss, P., J. Bleuse, *Nano Lett.* **2**, (2002) 781-784.
- [22] Katari, J. E. B., V. L. Colvin, *J Phys. Chem.*, **98**, (1994) 4109-4117.
- [23] D. Gerion, F. Pinaud, S. C. Williams, *J Phys. Chem. B*, **105**, (2001) 8861–8871.
- [24] Correa-Duarte, M. A., M. Giersig., *Chem. Phys. Lett.* **286**, (1998) 497.
- [25] Atsushi Ishizumi, Emiko Jojima, Aishi Yamamoto, and Yoshihiko Kanemitsu, *J. Phys. Soc. Jpn.* **77**, (2008) 053705.
- [26] Kumbhojkar, V.V.Nikesh, A.Kshirsagar, *Journal of Applied Physics*, **88**,

- (2000) 11.
- [27] K. Manzoor, S. R. Vadera, N. Kumar and T. R. N. Kutty, Solid State Communications, **129**, (2004) 469-473.
- [28] Gopa Ghosh, Milan Kanti, Naskar, Amitava Patra, Minati Chatterjee, Journal of Optical Materials, **28**, (2006) 1047-1053.
- [29] Rajesh Sharma, H S Bhatti, Nanotechnology, **18**, (2007) 465703(7pp).